NREL entrained flow reactor

Gavin Wiggins

May 13, 2020

Contents

1 Introduction

This report provides an overview of the Entrained Flow Reactor (EFR) at NREL. The reactor operates at fast pyrolysis conditions to thermochemically convert biomass into gaseous products. The EFR is part of the Thermochemical Process Development Unit (TCPDU) at NREL which was originally designed for biomass gasification where the EFR was used as a thermal cracker. An overview of the TCPDU system is shown in Figure 1.

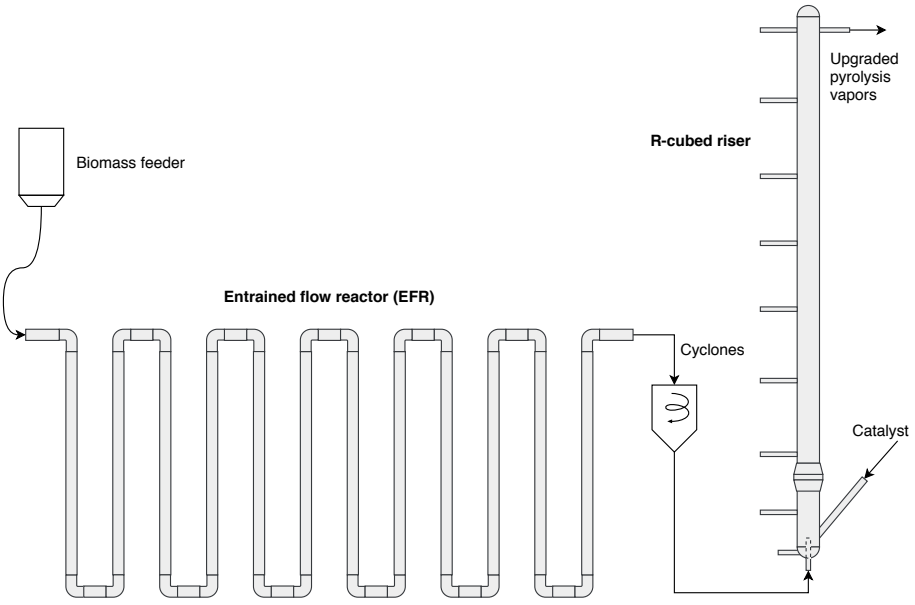

Figure 1: Overview of the main components of the NREL TCPDU system. Fast pyrolysis of biomass occurs in the entrained flow reactor. Catalytic vapor phase upgrading occurs in the R-cubed riser reactor.

2 Entrained flow reactor (EFR)

The following sections provide geometric dimensions and process flow information for the entrained flow reactor (EFR). Computational model results are also presented in this section.

2.1 Experimental setup

Fast pyrolysis in the TCPDU system occurs in the entrained flow reactor (pictured in Figure 2) which is comprised of a series of horizontal and vertical pipes connected with 90 degree elbows. Dimensions and material information about the EFR are provided in Figure 3 below. Operating conditions such as temperatures, pressures, and flow rates for the EFR are shown in Figure 4. Nitrogen gas at 500°C is used as the conveying medium for the solids.

2.2 Residence time distribution

Ideally, experimental measurements are used to develop a residence time distribution (RTD) curve of the solids in a fluidized system. However, the reactor systems at NREL are not equipped to measure solids residence time therefore computational reactor models were developed to determine this information for

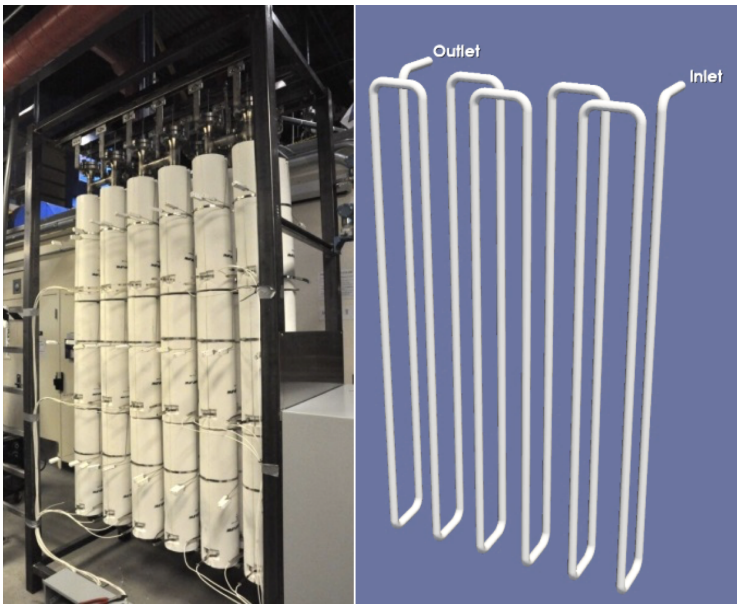

Figure 2: Left - picture of the EFR assembly with heat jackets, insulation, and thermocouples. Right - CAD representation of the EFR pipe assembly used for MFiX simulations.

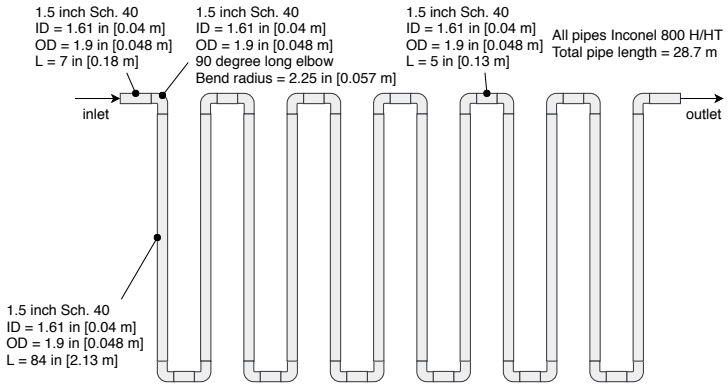

Figure 3: Geometry of the entrained flow reactor at NREL.

the particle-scale simulations. The residence time distributions were determined from MFiX simulations of spheres at various particle sizes with a N_2 carrier gas velocity of 4.78 m/s and a solids mass flow rate of 15 kg/s. The EFR is essentially a pneumatic conveyor where biomass particles flow through a long pipe with several bends. The CAD representation of the EFR used for the MFiX residence time simulations is shown in Figure 2.

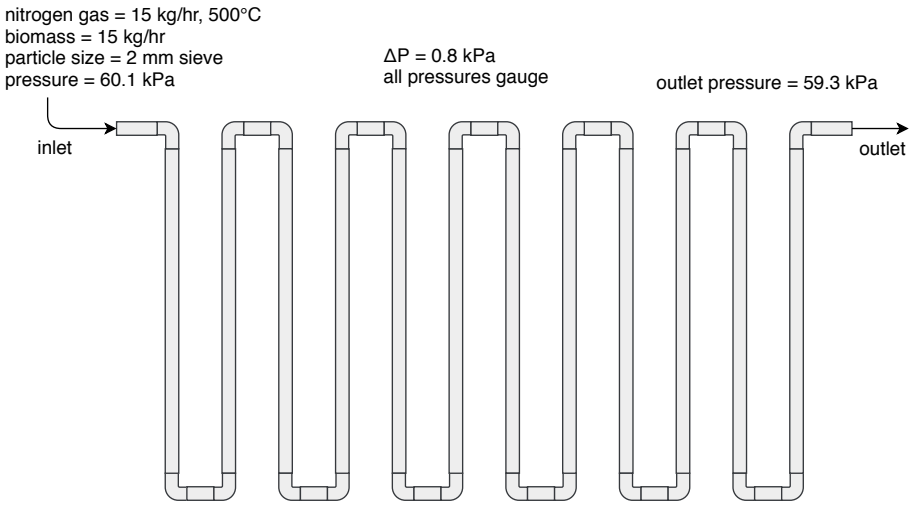

Figure 4: Typical operating conditions for the entrained flow reactor.

By using a discrete element model (DEM) in MFiX we can track individual particles in the reactor and determine when they leave the system. The DEM simulation was populated with two thousand particles comprised of five different sizes that were initially placed at the inlet of the reactor to simulate a pulse-tracer experiment. An initial gas flow rate and pressure drop are imposed along the reactor to allow the system to quickly attain steady state conditions. A gas phase boundary condition is established at the reactor entrance pushing 15 kg/hr of hot nitrogen gas through the system to reach solids fluidization. A pressure outlet boundary condition was set up at the reactor exit to allow particles and gas to flow out of the system. The particles are tracked as they move over time and their reactor exit time is recorded. The DEM simulation with particles after three seconds in the reactor is shown in Figure 5.

After simulation setup, it takes approximately four weeks of computation time on a single-core machine for all particles to leave the reactor. Using the recorded exit time of each particle, the concentration of particles exiting the reactor at a given time step is calculated. From this information, a concentration profile and associated exit age distribution for a given particle size distribution is developed for the EFR. The concentration and residence time distribution curve for the solids in the entrained flow reactor is shown in Figure 6. It should be noted that at the time of this report, simulations using the particle measurements from Microtrac were still running. Therefore, to improve the results of the particle-scale pyrolysis model, the revised RTD should be incorporated into future models.

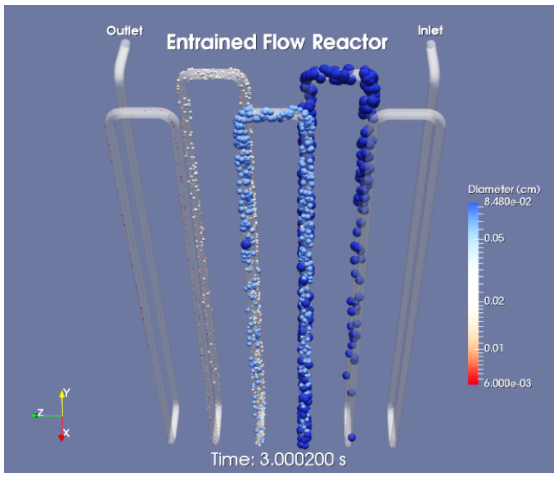

Figure 5: Entrained flow reactor after approximately three seconds. Particle diameters are scaled 50x for visualization purposes.

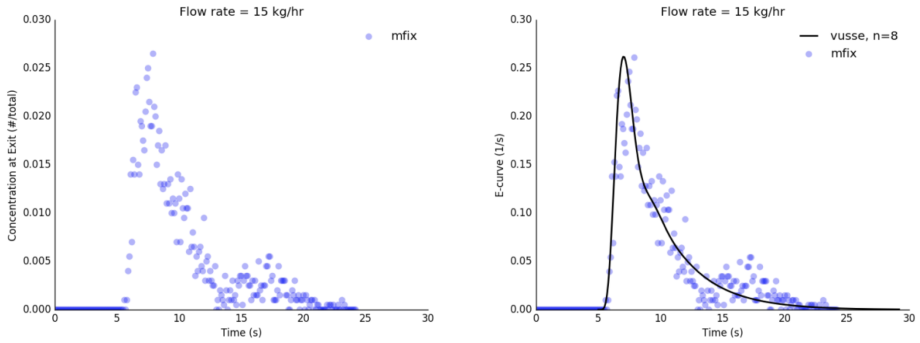

Figure 6: Concentration of oak particles leaving EFR (left). Residence time distribution calculated from concentration profile (right). Reactor conditions 500°C with 15 kg/s solids and gas flow. The solid line (right) represents the Van de Vusse correlation for estimating the number of CSTRs that represent mixing in the system.

2.3 Biomass pyrolysis kinetics

The Ranzi et al. kinetic scheme for biomass fast pyrolysis is described in this section.

Table 1: Solid species in Ranzi kinetic scheme.

Item	Abbreviation	Name	Formula
1	CELL	cellulose	$C_6H_{10}O_5$
2	CELLA	activated cellulose	$C_6H_{10}O_5$
3	CHAR	char	C
4	GCO	metaplastic carbon monoxide	CO
5	GCO2	metaplastic carbon dioxide	CO_2
6	GCH4	metaplastic methane	CH_4
7	GC2H4	metaplastic ethylene	C_2H_4
8	GCH3OH	metaplastic methyl alcohol	CH_4O
9	GCOH2	metaplastic formaldehyde	CH_2O
10	GH2	metaplastic hydrogen	H_2
11	GMSW	hemicellulose softwood	$C_5H_8O_4$
12	HCE1	hemicellulose	$C_5H_8O_4$
13	HCE2	hemicellulose	$C_5H_8O_4$
9	HMWL	heavy molecular weight lignin	$C_{24}H_{28}O_4$
14	LIG	lignin	$C_{11}H_{12}O_4$
15	LIGC	lignin carbon	$C_{15}H_{14}O_4$
16	LIGCC	lignin carbon	$C_{15}H_{14}O_4$
17	LIGH	lignin hydrogen	$C_{22}H_{28}O_9$
18	LIGO	lignin oxygen	$C_{20}H_{22}O_{10}$
19	LIGOH	lignin hydroxide	$C_{19}H_{22}O_8$
20	XYHW	hemicellulose hardwood	$C_5H_8O_4$

Table 2: Gas species in Ranzi kinetic scheme.

Item	Abbreviation	Name	Formula
1	ACAC	acetic acid	$C_2H_4O_2$
2	ALD3	propanal	C_3H_6O
3	ANISOLE	anisole	C_7H_8O
4	C2H4	ethylene	C_2H_4
5	C2H6	ethane	C_2H_6
6	C2H5OH	ethanol	C_2H_6O
7	C2H3CHO	2-propenal	C_3H_4O
8	C3H6O2	propanal, 3-hydroxy-	$C_3H_6O_2$
9	CH2O	formaldehyde	CH_2O
10	CH3OH	methyl alcohol	CH_4O
11	CH3CHO	acetaldehyde	C_2H_4O
12	CH4	methane	CH_4
13	CO	carbon monoxide	CO
14	CO2	carbon dioxide	CO_2
15	COUMARYL	coumaryl alcohol	$C_9H_{10}O_2$
16	FE2MACR	sinapaldehyde	$C_{11}H_{12}O_4$
17	FURF	furfural	$C_5H_4O_2$
18	GLYOX	glyoxal	$C_2H_2O_2$
19	H2	hydrogen	H_2
20	H2O	water	H_2O
21	HAA	hydroxy-acetaldehyde	$C_2H_4O_2$
22	HCOOH	formic acid	CH_2O_2
23	HMFU	5-hydroxymethyl-furfural	$C_6H_6O_3$
24	LVG	levoglucosan	$C_6H_{10}O_5$
25	PHENOL	phenol	C_6H_6O
26	XYLAN	xylosan	$C_5H_8O_4$

3 Blend3 feedstock

This section provides information about the "Blend3" feedstock as used for the FCIC project. See the sections below for general information, chemical composition, particle characterization, and reactor experiments associated with this feedstock.

3.1 Information

Table 3: General information for the Blend3 feedstock.

Item	Description
Name	Blend3
ID	?
Contact	?

3.2 Proximate and ultimate analyses

Table 4: Blend3 proximate analysis mass percent, as-received basis. Source [3].

Proximate	% ar	% ar	% ar
FC	16.92	?	?
VM	76.40	?	?
ash	0.64	?	?
moisture	6.04	?	?

Table 5: Blend3 ultimate analysis mass percent, as-received basis. Source [3].

Element	% ar	% ar	% ar
C	49.52	?	?
H	5.28	?	?
O	38.35	?	?
N	0.15	?	?
S	0.02	?	?
ash	0.64	?	?
moisture	6.04	?	?

3.3 Chemical analysis

The chemical components listed below are grouped into cellulose, hemicellulose, lignin, tann, tgl, and ash for use in the Debiagi 2018 biomass pyrolysis kinetics [4]. Celluluse is represented by glucan. Hemicellulose is acetyl, arabinan, galactan, mannan, and xylan. Tannins (TANN) are represented by free fructose, free glucose, sucrose, and water extractives while triglycerides (TGL) are ethanol extractives. Ash is the non-structural and structural inorganics.

Table 6: Blend3 chemical composition analysis mass percent, dry basis. Components are grouped into cellulose, hemicellulose, lignin, tann, and tgl for use in the Debiagi pyrolysis kinetics. Source [6].

Chemical component	Group	% dry	% dry	% dry
glucan	cellulose	38.95	?	?
acetyl	hemicellulose	1.59	?	?
arabinan	hemicellulose	1.40	?	?
galactan	hemicellulose	3.16	?	?
mannan	hemicellulose	10.52	?	?
xylan	hemicellulose	7.89	?	?
lignin	lignin	29.48	?	?
free fructose	tann	0.07	?	?
free glucose	tann	0.04	?	?
sucrose	tann	0.04	?	?
water extractives	tann	2.75	?	?
ethanol extractives	tgl	3.49	?	?
non-structural inorganics	ash	0.22	?	?
structural inorganics	ash	0.41	?	?

Table 7: Blend3 biomass composition mass percent, dry basis. Values are calculated from Table 6.

Biomass composition	% dry
cellulose	38.95
hemicellulose	24.56
lignin	29.48
tann	2.90
tgl	3.49
ash	0.63

Table 8: Blend3 ash analysis as weight percent of ash. Source [3].

Metal oxide	wt. %	wt. %	wt. %
SiO_2	28.1	?	?
Al_2O_3	7.06	?	?
TiO_2	0.34	?	?
CaO	21.8	?	?
Na_2O	0.71	?	?
K_2O	13.8	?	?
P_2O_5	5.47	?	?
SO_3	1.23	?	?
Cl	0.09	?	?
CO_2	5.14	?	?

3.4 Particle characterization

Table 9: Blend3 particle properties from pelletized crushed feedstock. The crushed feedstock is used in the entrained flow reactor.

Property	Value	Description	Source
ρ	1,050 kg/m^3	particle density, daf basis	[5]
η	0.27	particle porosity	
k	0.23 W/mK	thermal conductivity	

3.5 Reactor yields

Table 10: Entrained flow reactor yields for Blend3 feedstock.

Yield	wt. %
total liquid	64.9
char	13.9 ± 0.1
gas	17.2 ± 0.2
mass balance	96.9 ± 1.5
carbon balance	93.0 ± 1.0

4 Forest residue feedstock

The forest residue feedstock is comprised of branches/twigs, cambium, needles, bark, and whitewood. This feedstock is used in the NREL fluidized bed reactor (FBR) for the purposes of the FCIC project. The FBR is operated at fast pyrolysis conditions for the thermochemical conversion of biomass. The reactor is sometimes referred to as the 2FBR.

4.1 Information

Table 11: General information for the forest residue feedstock.

Item	Description
Name	forest residue
ID	?
Contact	?

4.2 Ultimate analysis

Table 12: Bark ultimate analysis mass percent, dry ash-free basis. Source [1].

Element	% daf	% daf	% daf
C	48.27	?	?
H	5.72	?	?
N	0.52	?	?

Table 13: Branches/twigs ultimate analysis mass percent, dry ash-free basis. Source [1].

Element	% daf	% daf	% daf
C	49.69	?	?
H	6.36	?	?
N	0.25	?	?

Table 14: Cambium ultimate analysis mass percent, dry ash-free basis. Source [1].

Element	% daf	% daf	% daf
C	48.52	?	?
H	6.39	?	?
N	0.11	?	?

Table 15: Needles ultimate analysis mass percent, dry ash-free basis. Source [1].

Element	% daf	% daf	% daf
C	48.59	?	?
H	5.92	?	?
N	1.22	?	?

Table 16: Whitewood ultimate analysis mass percent, dry ash-free basis. Source [1].

Element	% daf	% daf	% daf
C	48.27	?	?
H	6.15	?	?
N	0.10	?	?

4.3 Chemical analysis

Table 17: Whitewood biomass composition mass percent, dry basis. Source [2].

Component	% dry
Cellulose	38.04
Hemicellulose	24.2

References

[1] Unknown Author. *CHN Analysis Report*. Tech. rep. From Excel spreadsheet `jw-pine-chn-report-jw190920`. Unknown institution, 2019.

[2] Unknown Author. *Summary normalized*. Tech. rep. From Excel spreadsheet `summary-normalized`. Unknown institution, 2020.

[3] Mike Choratch. *Proximate and ultimate analysis*. Tech. rep. From PDF `chns_ipc_ms_blend3_nrel2017`. Hazen Research, Inc, 2017.

[4] P. Debiagi et al. "A predictive model of biochar formation and characterization". In: *Journal of Analytical and Applied Pyrolysis* 134 (2018), pp. 326–335.

[5] M. Brennan Pecha et al. "Integrated Particle- and Reactor-Scale Simulation of Pine Pyrolysis in a Fluidized Bed". In: *Energy & Fuels* 32.10 (2018), pp. 10683–10694.

[6] Anne Starace and Justin Sluiter. *Compositional analysis Blend3*. Tech. rep. From Excel spreadsheet `comp_analysis_blend3_fy17verification`. National Renewable Energy Laboratory, 2020.